



Last Time

- Bubble departure frequency and diameter
- Different regimes in pool boiling
- Rohsenow's microconvection model for nucleate boiling



- Zuber's CHF model based on Helmholtz and Taylor instabilities
- Force balance model for CHF
- Effect of surface parameters on CHF
- Statistical approach for CHF



Helmholtz Instability of Vapor Columns

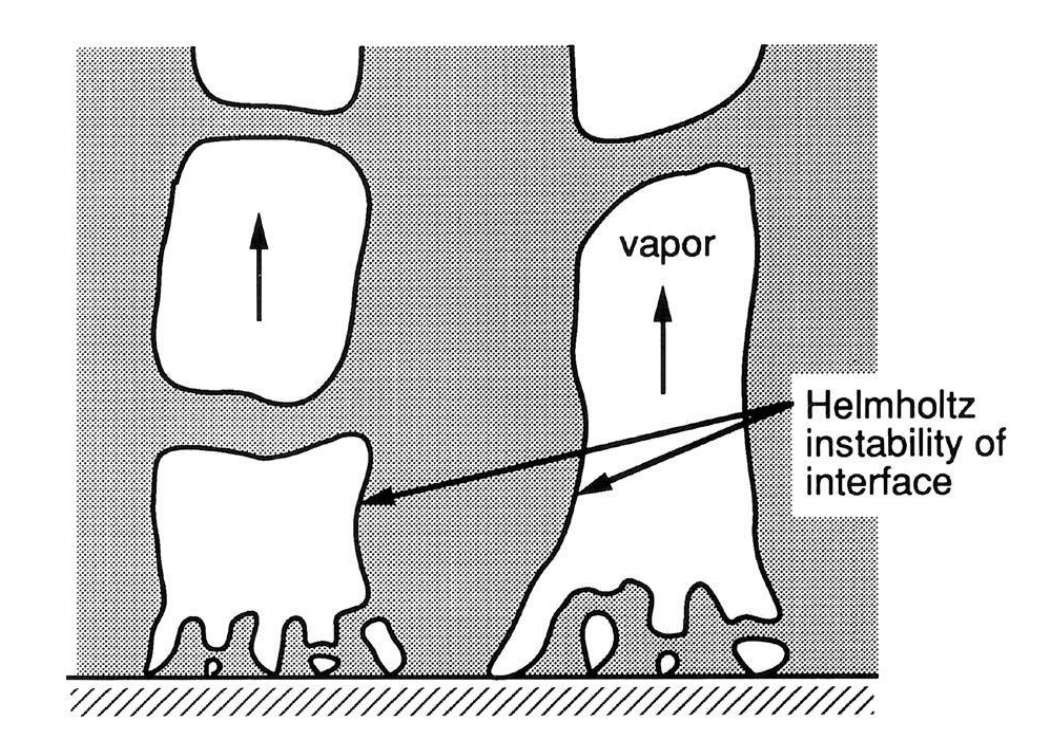


Figure 7.16 Carey



Video credit: Dr. Rameez Iqbal



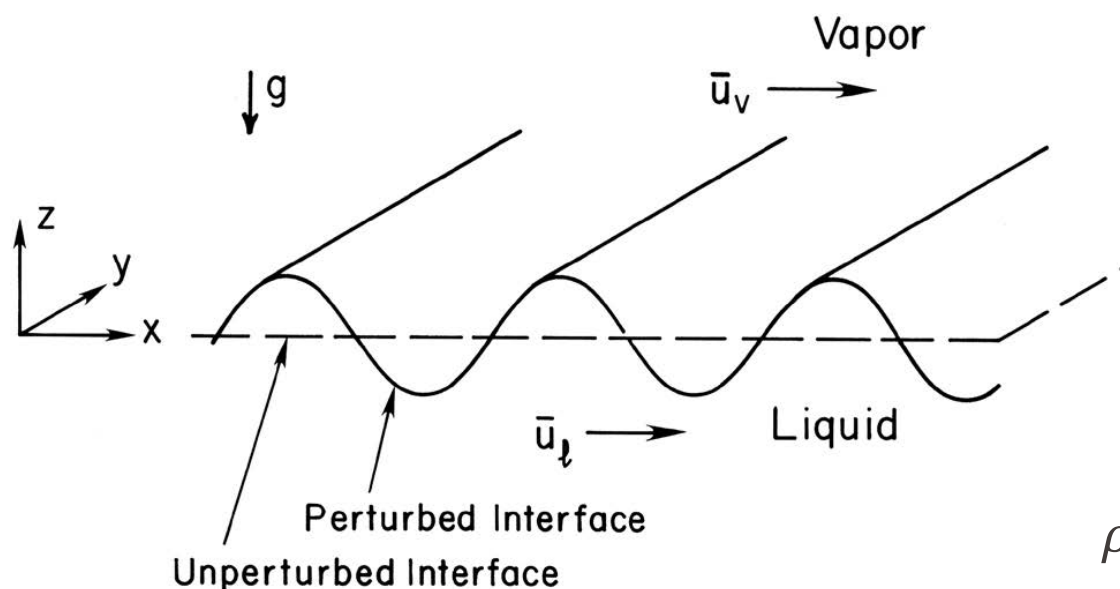


Figure 4.4 in Carey

Continuity

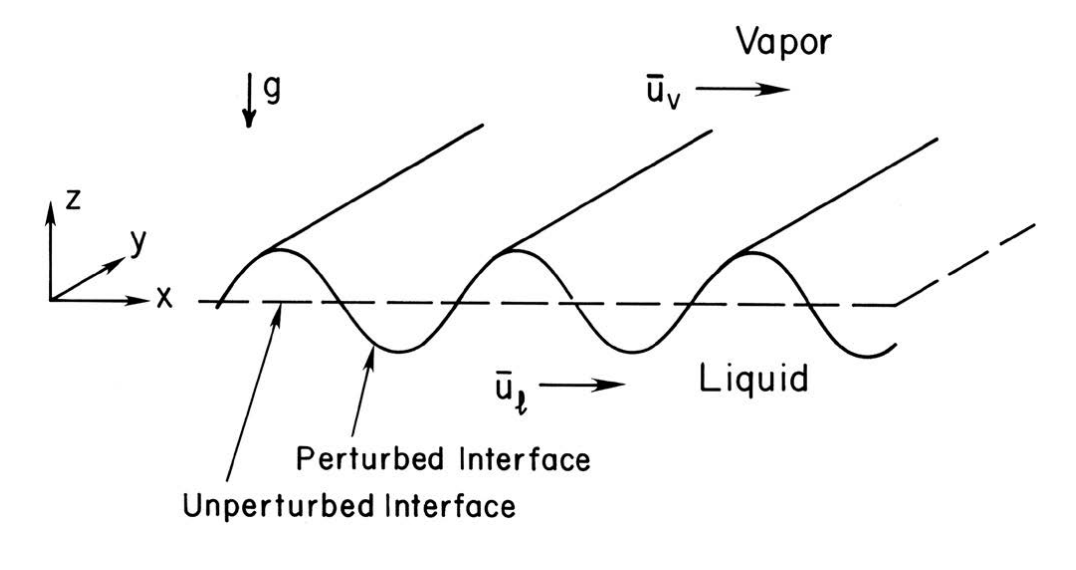
$$\frac{\partial u}{\partial x} + \frac{\partial w}{\partial z} = 0$$

Momentum balance (neglecting viscosity)

$$\rho \left(\frac{\partial u}{\partial t} + u \frac{\partial u}{\partial x} + w \frac{\partial u}{\partial z} \right) = -\frac{\partial P}{\partial x}$$

$$\rho \left(\frac{\partial w}{\partial t} + u \frac{\partial w}{\partial x} + w \frac{\partial w}{\partial z} \right) = -\frac{\partial P}{\partial z} - \rho g$$

Helmholtz Instability



Consider after a perturbation $\delta(x, t = 0) = Ae^{i\alpha x}$

$$u: \overline{u} \to \overline{u} + u', \qquad w: 0 \to w', \qquad P: \overline{P} \to \overline{P} + P'$$

$$\frac{\partial u'}{\partial x} + \frac{\partial w'}{\partial z} = 0$$

$$\rho\left(\frac{\partial u'}{\partial t} + \bar{u}\frac{\partial u'}{\partial x}\right) = -\frac{\partial P'}{\partial x}$$

$$\Rightarrow \frac{\partial^2 P'}{\partial x^2} + \frac{\partial^2 P'}{\partial z^2} = 0$$

$$\rho\left(\frac{\partial w'}{\partial t} + \bar{u}\frac{\partial w'}{\partial x}\right) = -\frac{\partial P'}{\partial z}$$

Postulate the form of the response function:

$$\delta = Ae^{i\alpha x + \beta t}$$

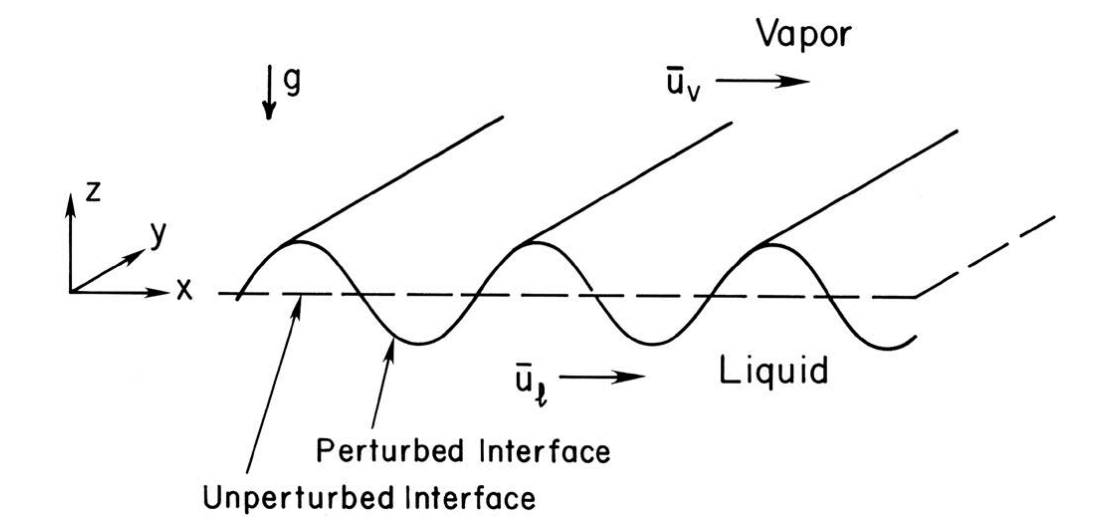
$$w' = \widehat{w}(z)e^{i\alpha x + \beta z}$$

$$w' = \widehat{w}(z)e^{i\alpha x + \beta t}$$
 $P' = \widehat{P}(z)e^{i\alpha x + \beta t}$

We are interested in β



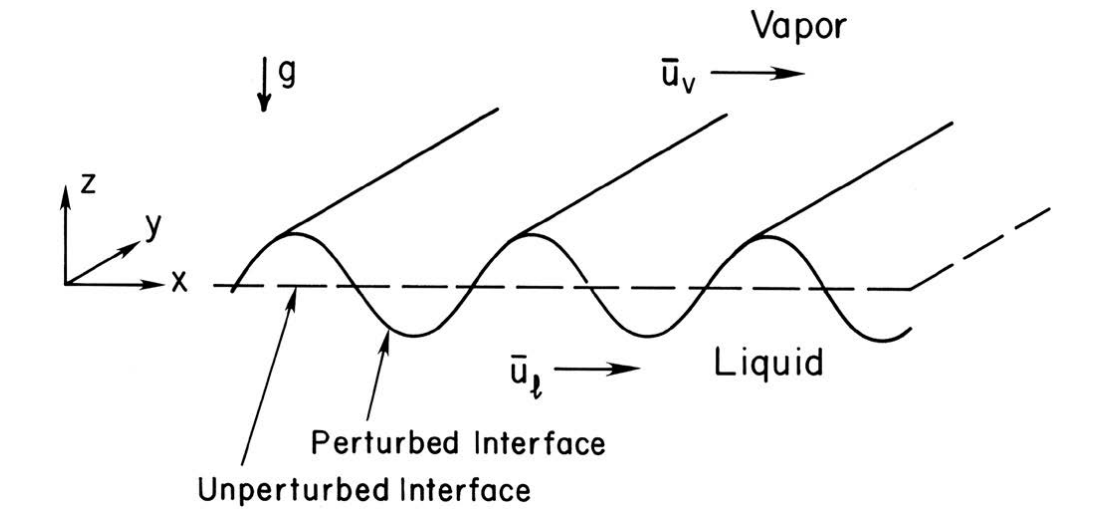
$$\frac{\partial^2 P'}{\partial x^2} + \frac{\partial^2 P'}{\partial z^2} = 0 \qquad P' = \hat{P}(z)e^{i\alpha x + \beta t}$$



$$w' = \widehat{w}(z)e^{i\alpha x + \beta t} \qquad \rho\left(\frac{\partial w'}{\partial t} + \overline{u}\frac{\partial w'}{\partial x}\right) = -\frac{\partial P'}{\partial z}$$



$$\frac{\partial u'}{\partial x} + \frac{\partial w'}{\partial z} = 0 \qquad w' = \widehat{w}(z)e^{i\alpha x + \beta t}$$



$$\delta = Ae^{i\alpha x + \beta t}$$

$$\widehat{w}_{v}(z) = \frac{a_{v}\alpha}{\rho_{v}(\beta + i\alpha\overline{u})}e^{-\alpha z}$$

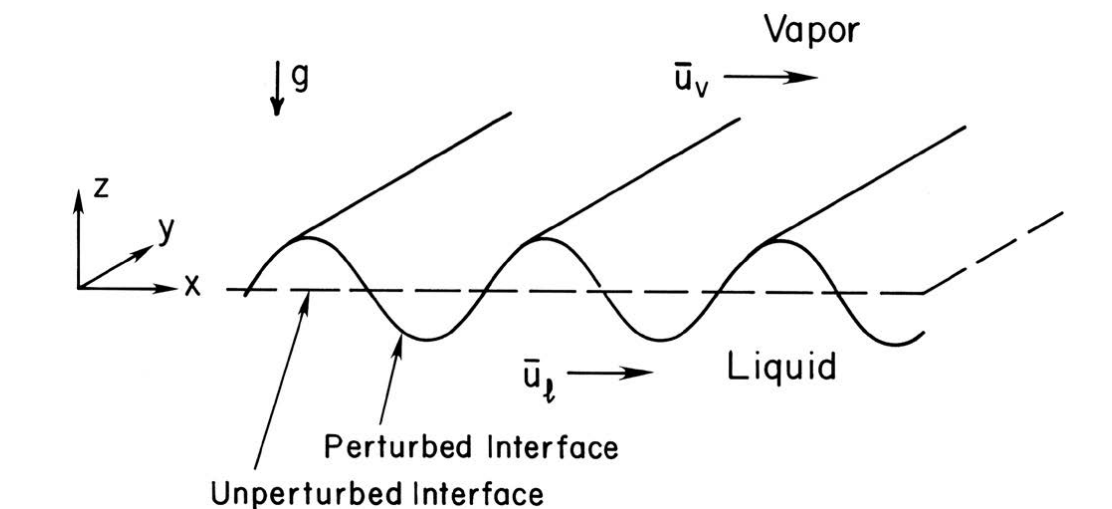
$$\widehat{w}_l(z) = -\frac{a_l \alpha}{\rho_l(\beta + i\alpha \overline{u})} e^{\alpha z}$$

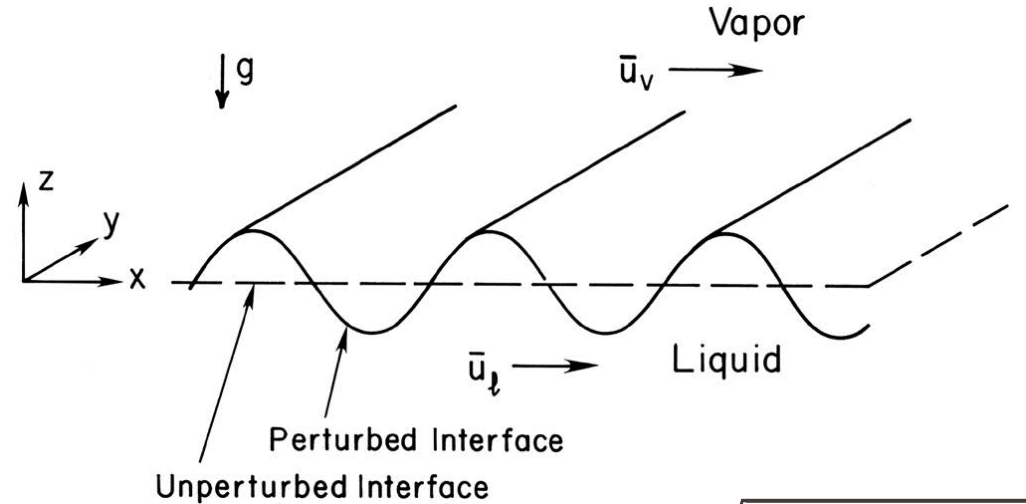


$$a_v = \frac{\rho_v}{\alpha} (\beta A + i\alpha \bar{u}_v)^2 A$$

$$a_l = -\frac{\rho_l}{\alpha} (\beta A + i\alpha \bar{u}_l)^2 A$$

$$\hat{P}_v = a_v e^{-\alpha z} \qquad \hat{P}_l = a_l e^{\alpha z}$$





Perturbation $\delta(x, t = 0) = Ae^{i\alpha x}$

$$\delta = Ae^{i\alpha x + \beta t}$$

$$w' = \widehat{w}(z)e^{i\alpha x + \beta t}$$

$$w' = \widehat{w}(z)e^{i\alpha x + \beta t}$$
$$P' = \widehat{P}(z)e^{i\alpha x + \beta t}$$

$$\beta = \pm \frac{\sqrt{\alpha^2 \rho_v \rho_l (\bar{u}_v - \bar{u}_l)^2 - (\sigma \alpha^3 + \Delta \rho g \alpha)}}{\rho_v + \rho_l} - i\alpha \frac{\rho_l \bar{u}_l + \rho_v \bar{u}_v}{\rho_v + \rho_l}$$

The perturbation will cause a growing response if and only if β has a positive real part

Instability condition:

$$|\bar{u}_v - \bar{u}_l| > \sqrt{\frac{\left(\sigma\alpha + \frac{\Delta\rho g}{\alpha}\right)(\rho_l + \rho_v)}{\rho_l\rho_v}}$$

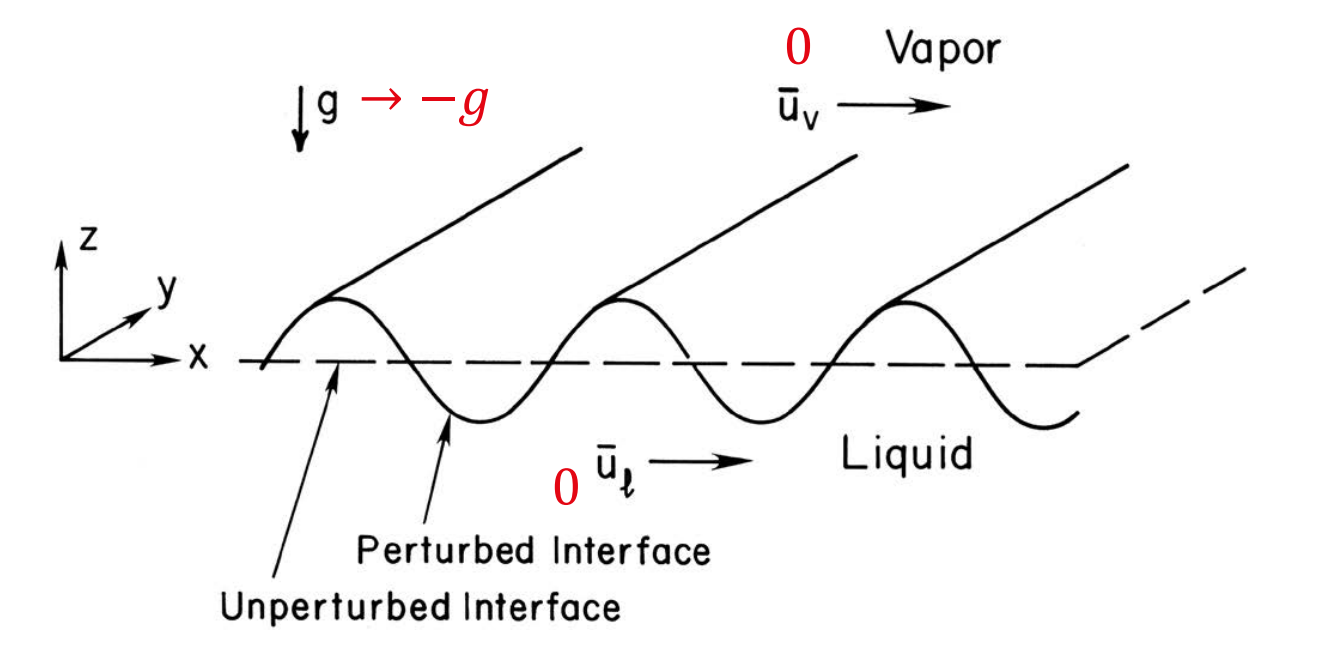
 $\bar{u}_{\nu} - \bar{u}_{l}$ promotes instability while gravity and surface tension suppressing instability, we can adjust the value of g based on the orientation of the system.







Taylor Instability



$$\delta = Ae^{i\alpha x + \beta t}$$

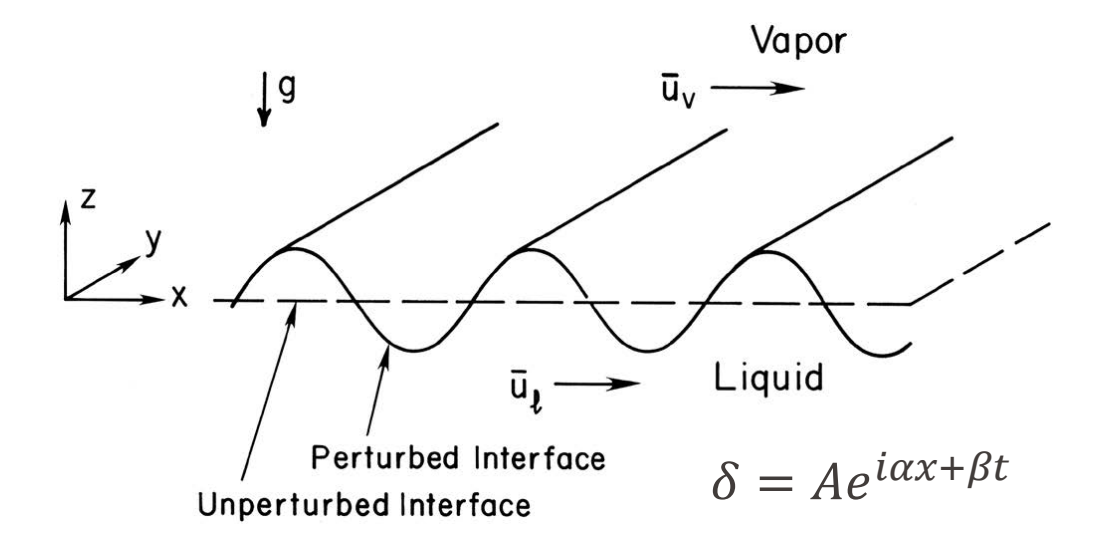
$$\beta = \pm \frac{\sqrt{\alpha^2 \rho_v \rho_l (\bar{u}_v - \bar{u}_l)^2 - (\sigma \alpha^3 + \Delta \rho g \alpha)}}{\rho_v + \rho_l} - i\alpha \frac{\rho_l \bar{u}_l + \rho_v \bar{u}_v}{\rho_v + \rho_l} \qquad \Rightarrow \beta = \pm \sqrt{\frac{\Delta \rho g \alpha - \sigma \alpha^3}{\rho_l + \rho_v}}$$

The fastest growing perturbation (α_{max}) in this case can be found by setting $\frac{d\beta}{d\alpha}=0$

The corresponding most dangerous wavelength $\lambda_D = \frac{2\pi}{\alpha_{max}} = 2\pi \sqrt{\frac{3\sigma}{\Delta\rho g}}$



How It's Related to Boiling



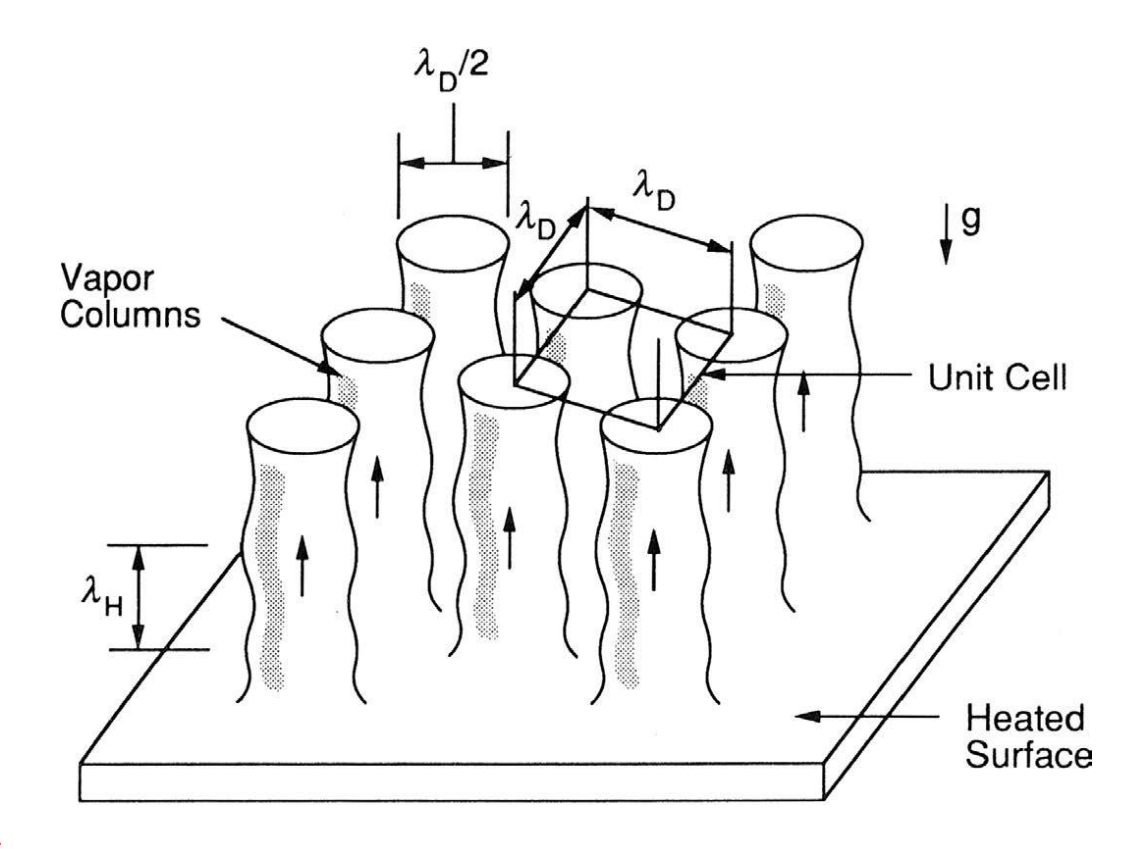
Helmholtz Instability

$$|\bar{u}_v - \bar{u}_l| > \sqrt{\frac{\left(\sigma\alpha + \frac{\Delta\rho g}{\alpha}\right)(\rho_l + \rho_v)}{\rho_l\rho_v}}$$

Setting g = 0 for vertical interfaces

$$|\bar{u}_v - \bar{u}_l| > \sqrt{\frac{\sigma\alpha (\rho_l + \rho_v)}{\rho_l \rho_v}} = \sqrt{\frac{2\pi\sigma (\rho_l + \rho_v)}{\rho_l \rho_v \lambda_H}} = u_c$$

Zuber's Model



- CHF is reached when interface of vapor columns becomes Helmholtz unstable (λ_H)
- The pitch of the vapor columns coincides with the most dangerous wavelength in Taylor instability

$$\lambda_D = 2\pi \sqrt{3\sigma/\Delta\rho g}$$

• The diameter of vapor column is $\lambda_D/2$

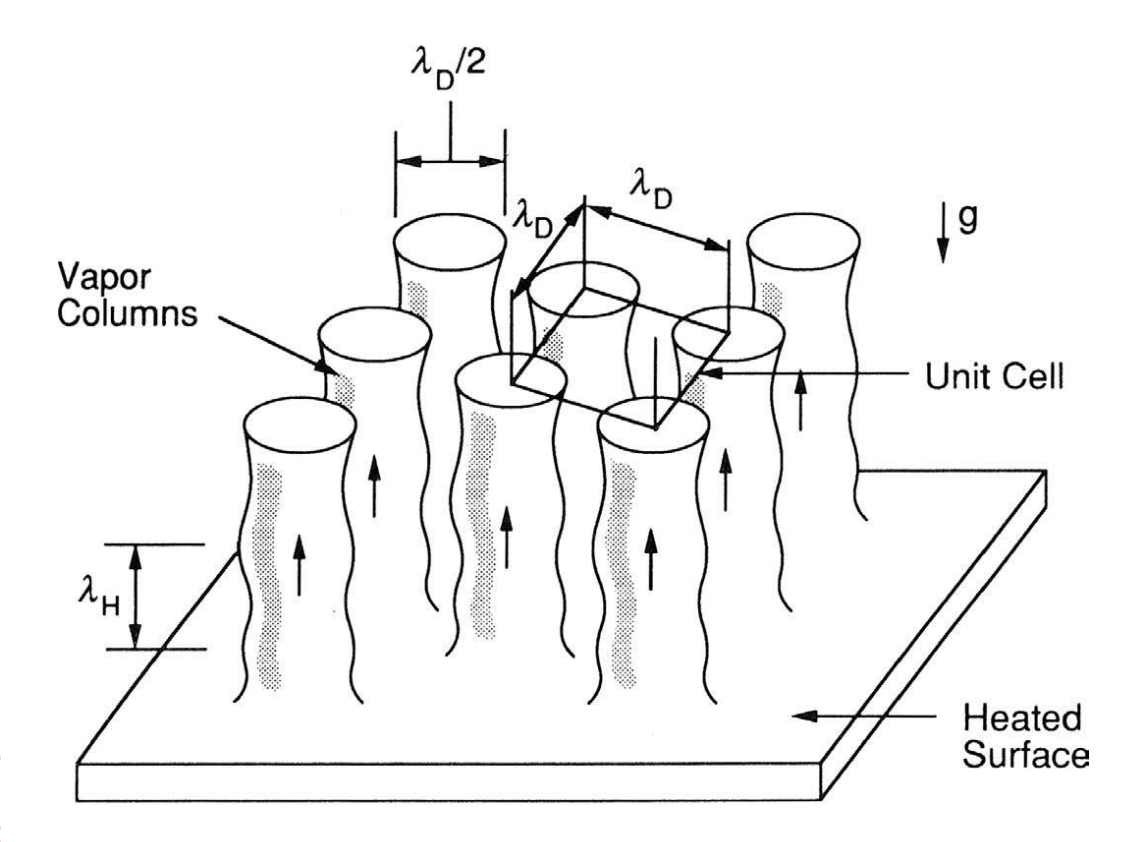
•
$$\lambda_H = \lambda_D \Rightarrow u_C = \sqrt{\frac{2\pi\sigma (\rho_l + \rho_v)}{\rho_l \rho_v \lambda_H}} \approx \sqrt{\frac{2\pi\sigma}{\rho_v \lambda_D}}$$



Zuber's Model

$$u_c = \sqrt{\frac{2\pi\sigma}{\rho_v \lambda_D}}$$

$$u_{c} = \sqrt{\frac{2\pi\sigma}{\rho_{v}\lambda_{D}}} \qquad \lambda_{D} = 2\pi\sqrt{\frac{3\sigma}{\Delta\rho g}}$$



$$u_c = \frac{q''_{max}}{\rho_v h_{lv}} \left(\frac{A_{surf}}{A_{col}}\right) = \frac{16}{\pi} \frac{q''_{max}}{\rho_v h_{lv}}$$

$$q_{max}^{"} = 0.149 \rho_v h_{lv} \left(\frac{\sigma \Delta \rho g}{\rho_v^2} \right)^{1/4}$$



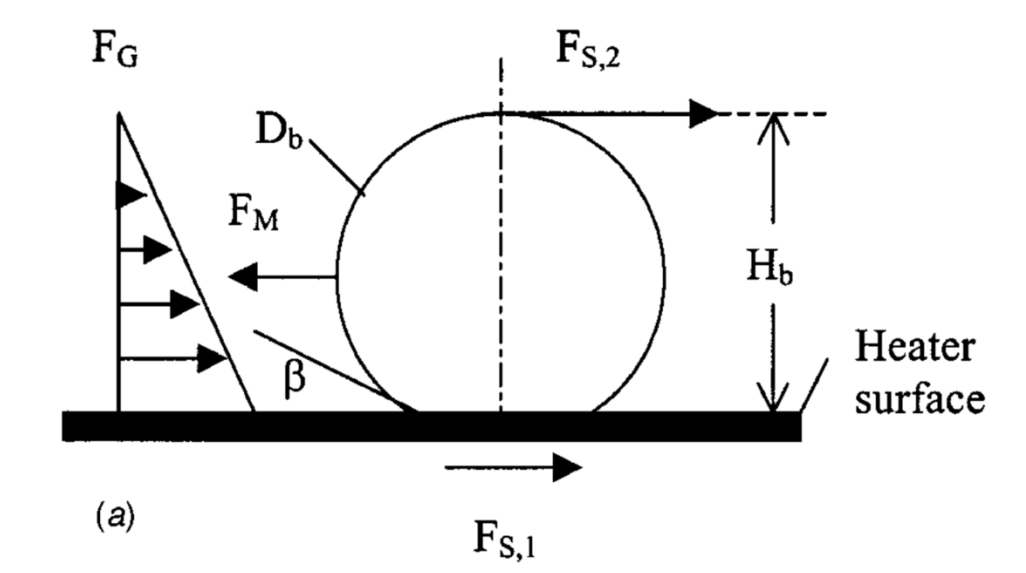
Comments on Zuber's Model

- No way to accommodate effects from geometry and surface wettability
- No clear justification for the choice of vapor column diameter as $\lambda_D/2$
- No visual observation of Helmholtz instability during boiling to date
- Still widely used as a reference model for all subsequence CHF models



Lateral Force Balance Model

https://doi.org/10.1115/1.1409265



Considering the lateral direction

Surface tension force : $F_{s,1}$, $F_{s,2}$

Hydrostatic force: F_G

Momentum force: F_M

Kandlikar suggested momentum balance requires $F_{S,1} + F_{S,2} + F_G = F_M$

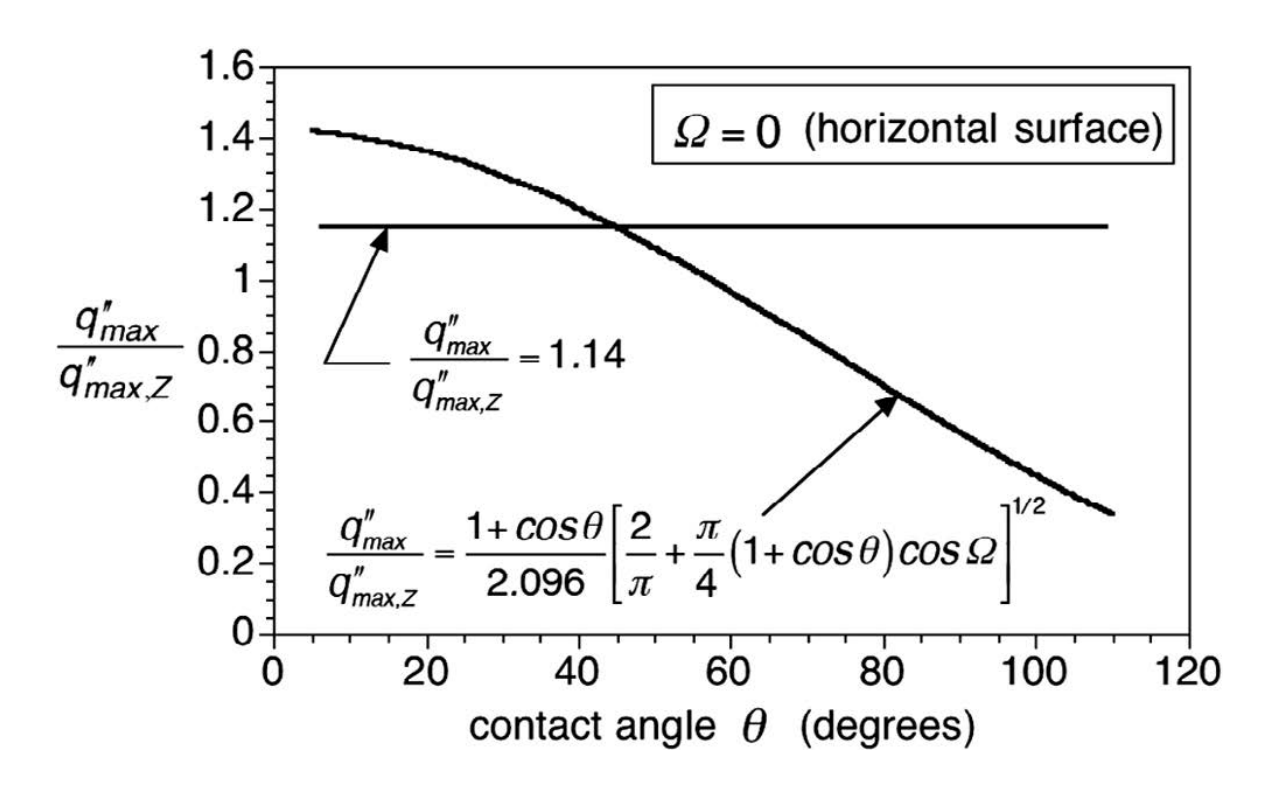
chose a bubble diameter at CHF $D_b = \lambda_D/2$ and set a bubble influence area πD_b^2

 λ_D : the most dangerous wavelength in Taylor instability



Contact Angle Dependence

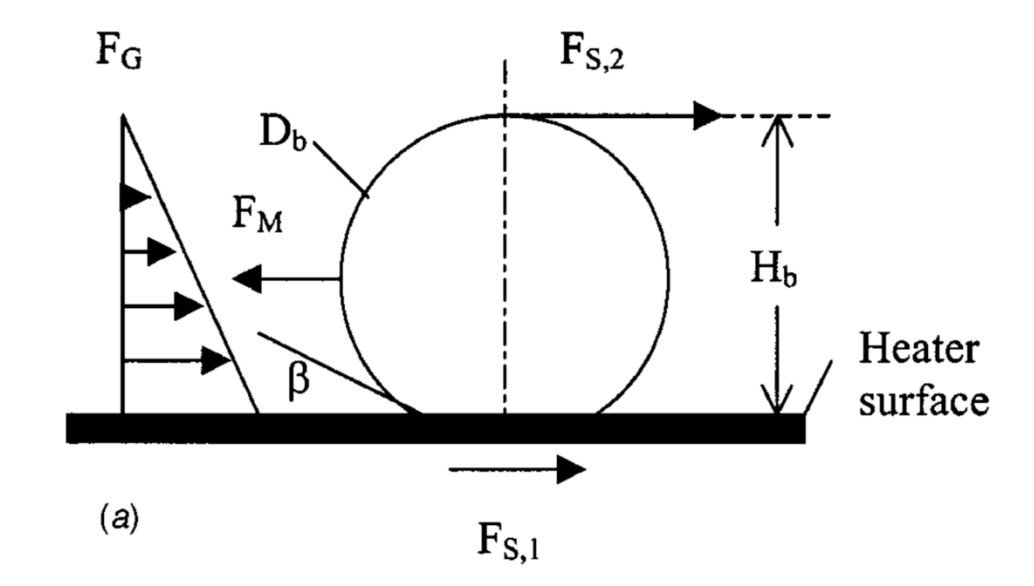
$$q_K'' = \rho_v h_{fg} \left(\frac{1 + \cos \beta}{16} \right) \left[\frac{2}{\pi} + \frac{\pi}{4} (1 + \cos \beta) \right]^{\frac{1}{2}} \left(\frac{\sigma \Delta \rho g}{\rho_v^2} \right)^{1/4}$$
 (Horizontal surface)



$$q_{max,Z}^{\prime\prime} = 0.149 \rho_v h_{lv} \left(\frac{\sigma \Delta \rho g}{\rho_v^2}\right)^{1/4}$$

$$\frac{q_K''}{q_{max,Z}''} = \frac{1 + \cos \theta}{2.096} \left[\frac{2}{\pi} + \frac{\pi}{4} (1 + \cos \beta) \right]^{\frac{1}{2}}$$

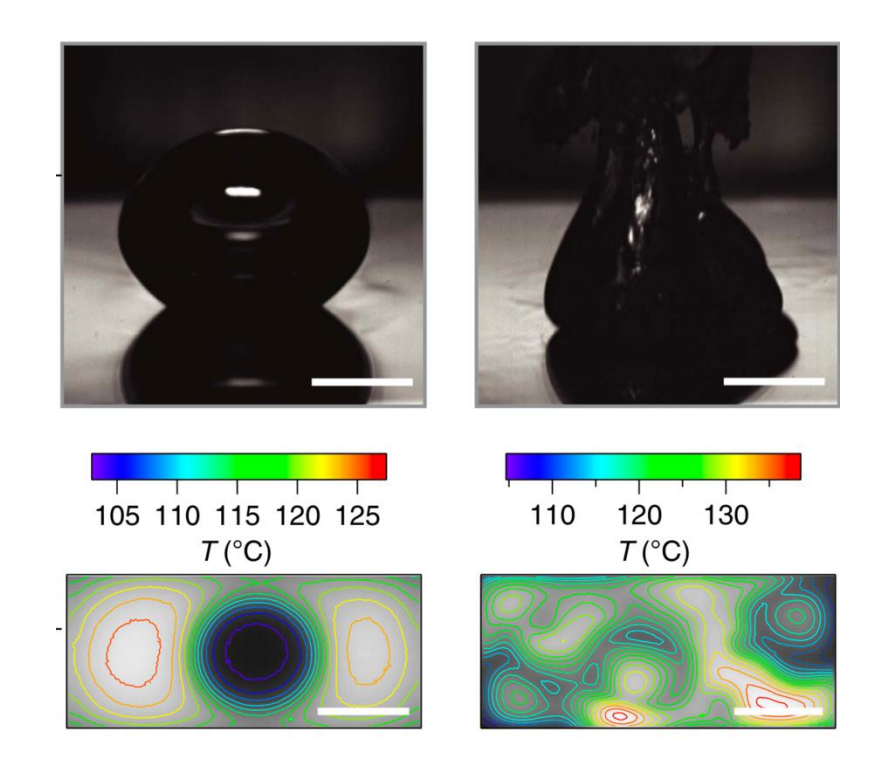
Comments on Kandlikar's Model



 $F_{S,1} + F_{S,2} + F_G = F_M$

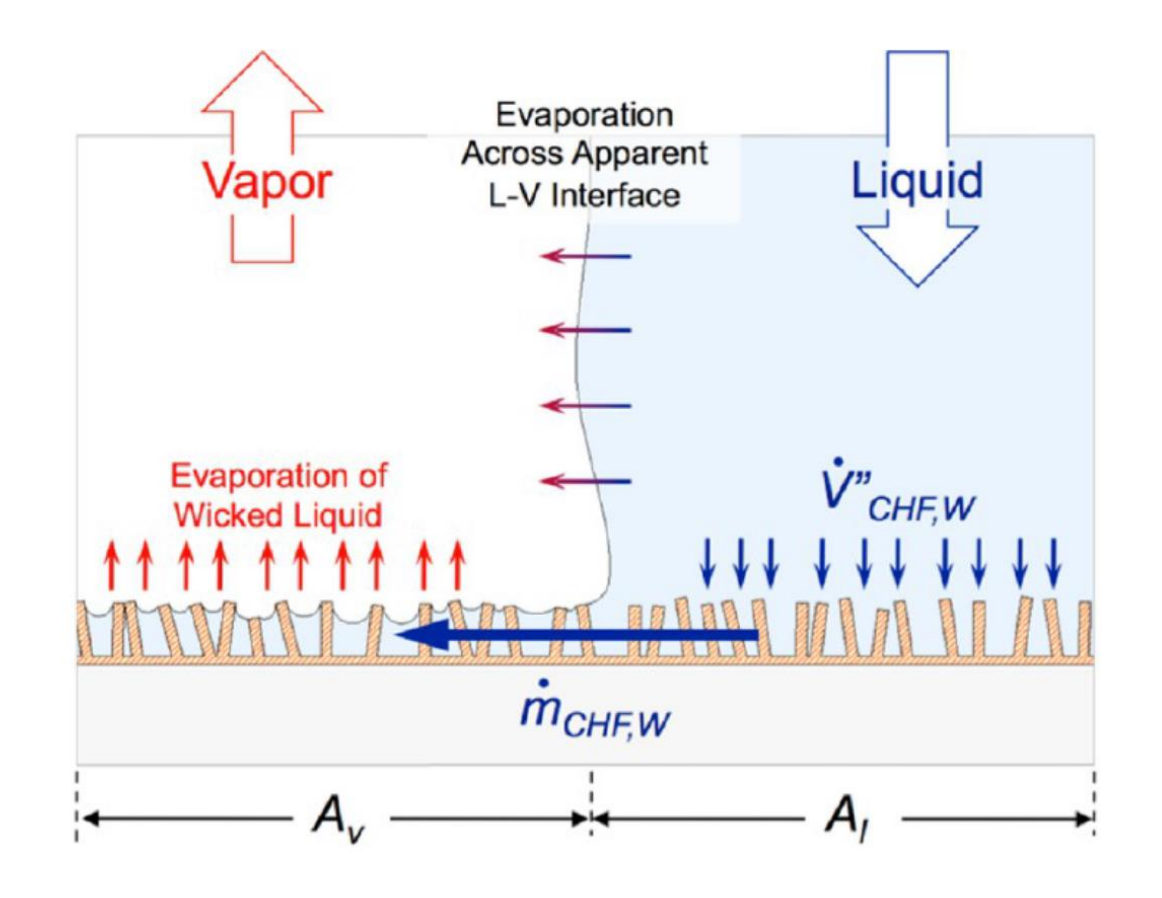
Liquid-vapor pressure difference not accounted for in momentum balance

Dhillon et al., Nat Commun 2015



Not clear how geometric parameters are chosen at CHF

Wicking Helps Boiling

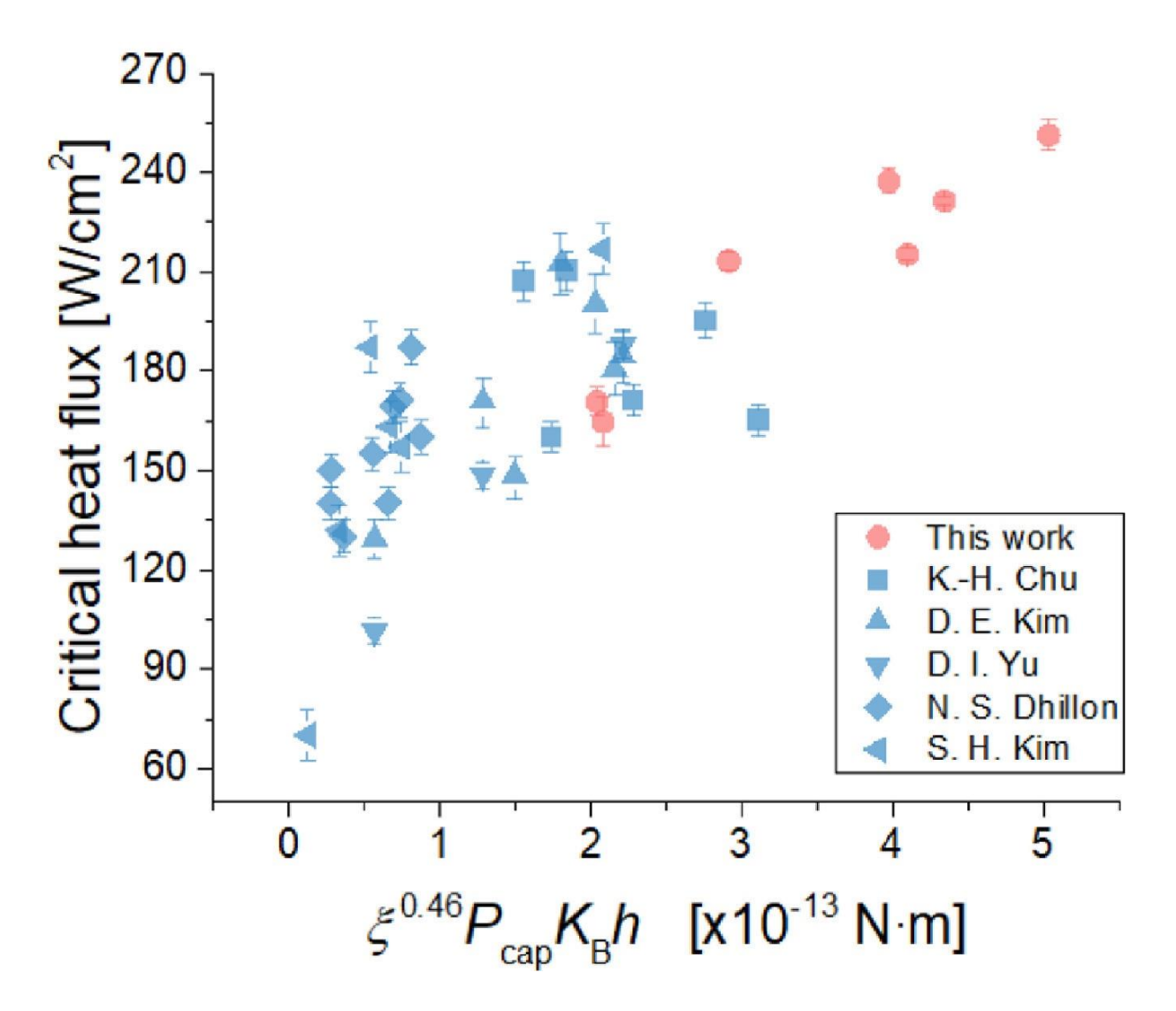




https://doi.org/10.1021/la5030923

https://doi.org/10.1021/acs.langmuir.7b01522

CHF vs Wicking on Hemispreading Surfaces



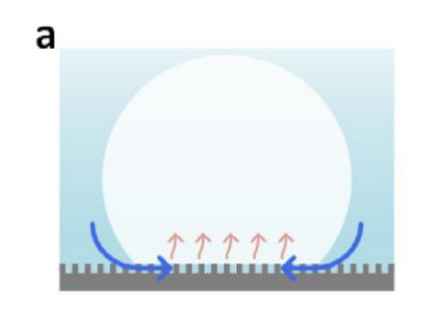
P_{cap}: capillary pressure

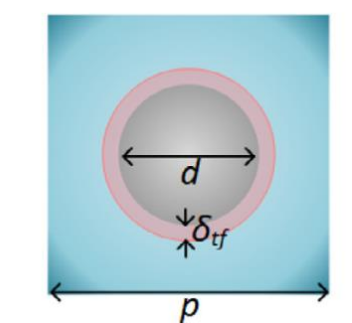
K_B: permeability

h: thickness of the wick

ξ: "thin film" liquid fraction

b



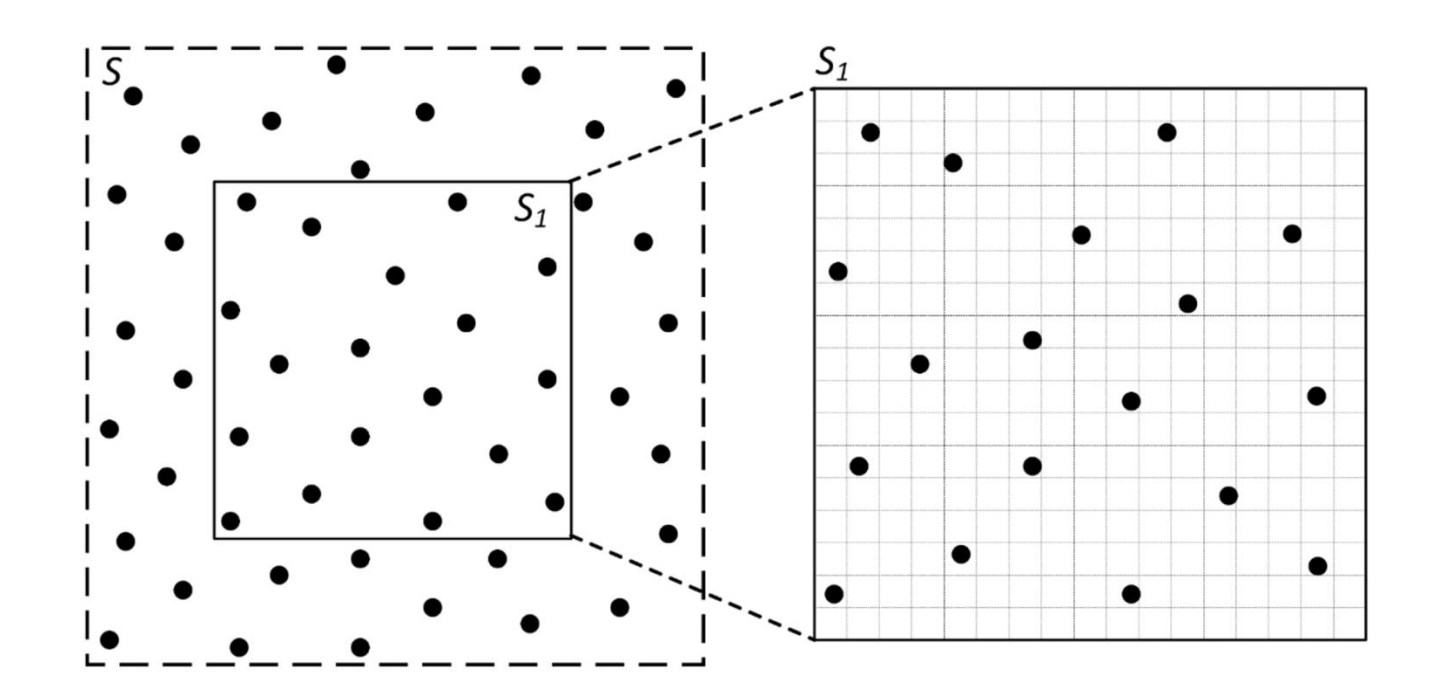




Statistical Approach for Flat Surface Boiling



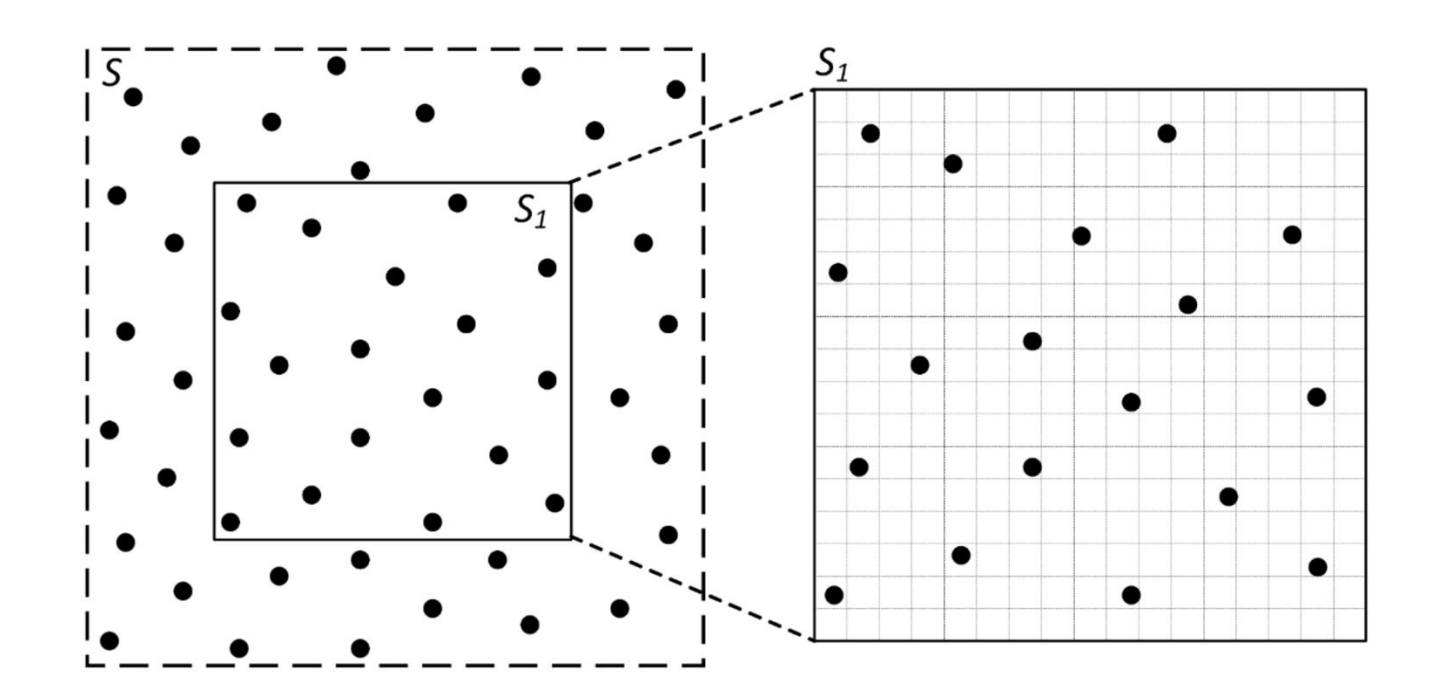




https://doi.org/10.1016/j.ijheatmasstransfer.2021.121904

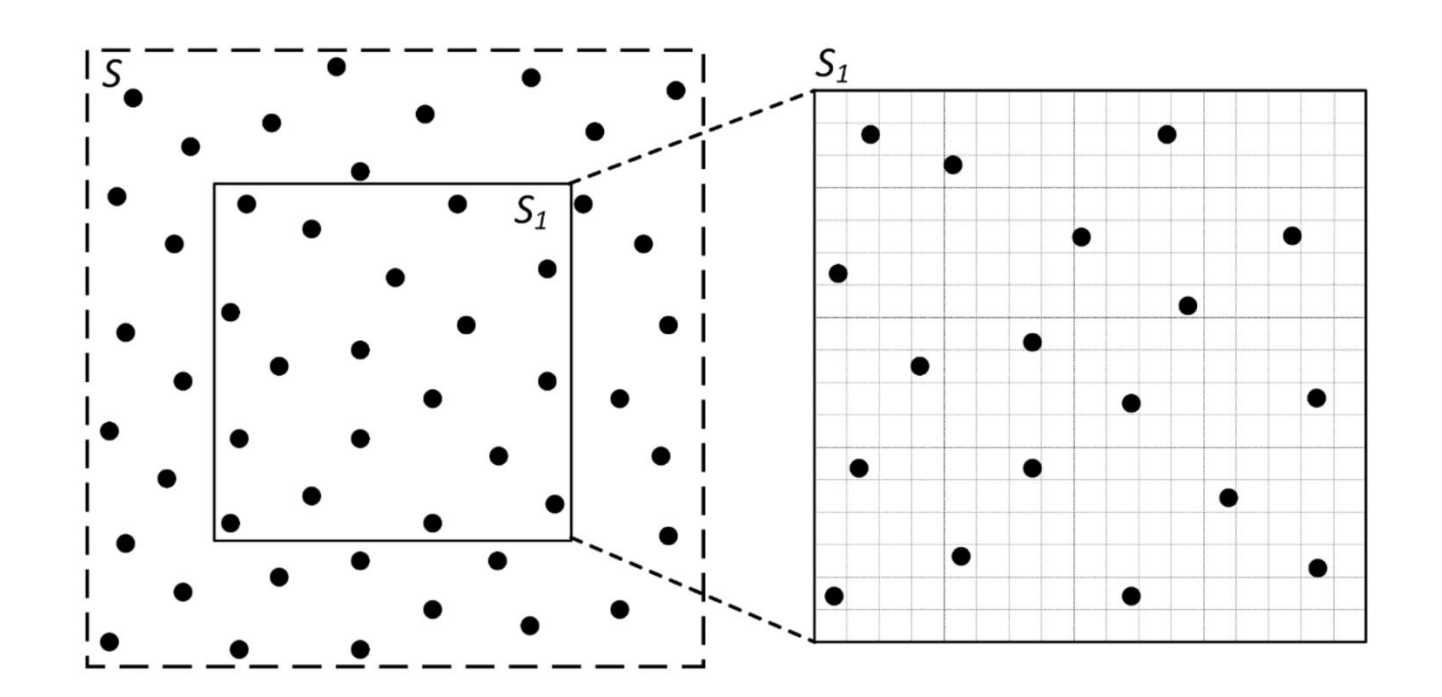
- Consider a large surface S (large enough to ignore edge effects)
- Probability of each point on the surface becoming an active nucleation sites is equal



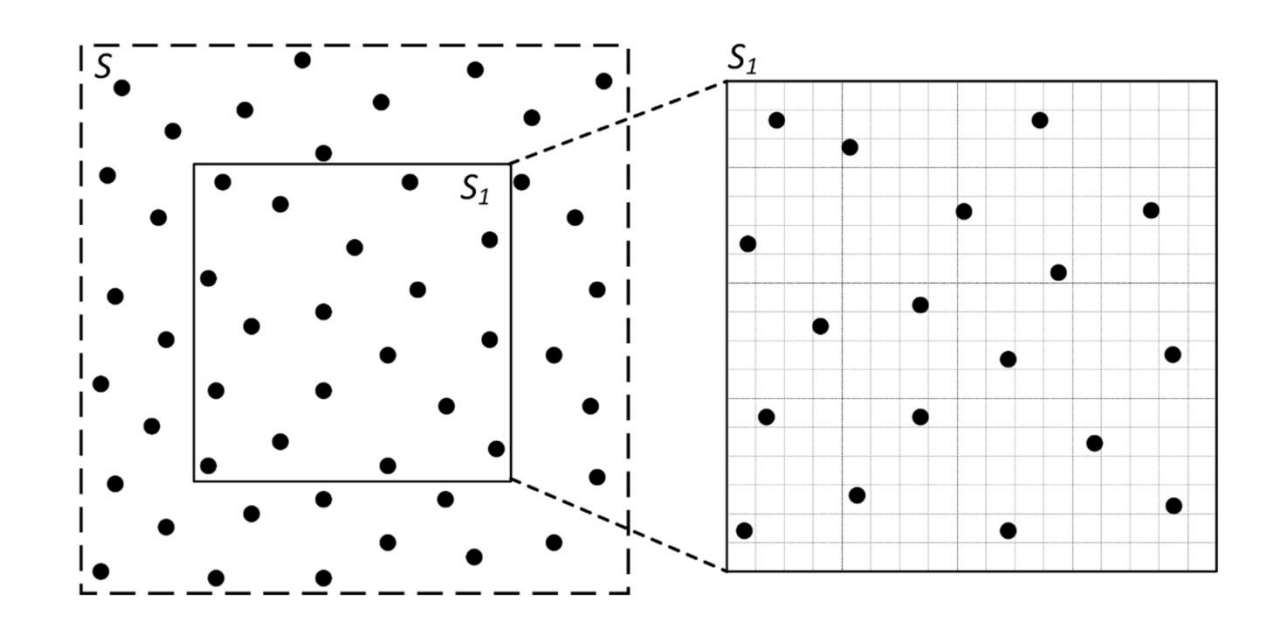


- Average nucleation density n_0 [m⁻²]
- For an arbitrary segment of the surface S_1 of area A, the average number of nucleation sites is $N_0 = n_0 A$
- The actual number of nucleation sites in S_1 , N_2 , is a random variable with an expectation value N_0



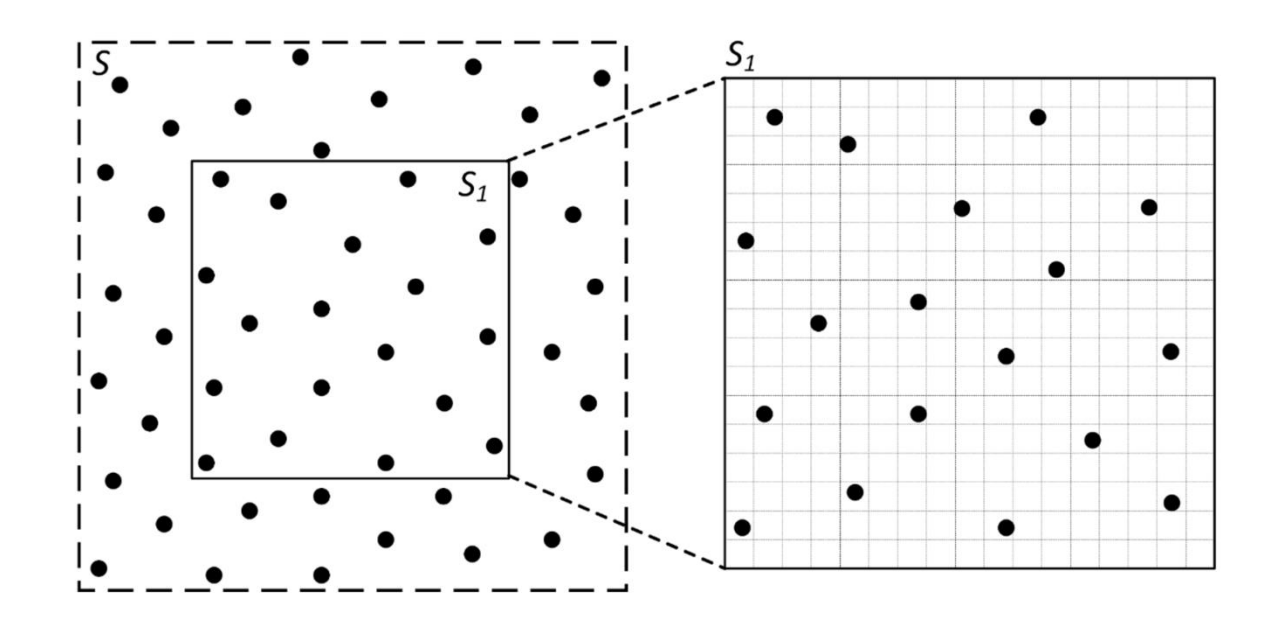


- Divide S₁ into M subsegments with the same area A/M
- Make M large enough such that the number of nucleation sites in each square is 0 or 1.
- Probability of finding a nucleation site in one square $p=N_0/M$



 Probability of find N squares that contain nucleation sites is a binomial distribution

$$P(N, N_0, M) = \frac{M!}{N! (M - N)!} p^N (1 - p)^{M - N}$$
$$= \frac{1}{N!} \cdot \frac{M!}{(M - N)! M^N} \cdot N_0^N \left(1 - \frac{N_0}{M}\right)^{M - N}$$



$$P(N, N_0, M) = \frac{1}{N!} \cdot \frac{M!}{(M - N)! M^N} \cdot N_0^N \left(1 - \frac{N_0}{M}\right)^{M - N}$$

Stirling's approximation: $\ln(n!) = n \ln n - n + O(\ln n)$ for $n \to \infty$

$$\lim_{M\to\infty}\ln\left[\frac{M!}{(M-N)!\,M^N}\right]=0\Rightarrow\lim_{M\to\infty}\frac{M!}{(M-N)!\,M^N}=1\qquad\qquad\lim_{M\to\infty}P\left(N,N_0,M\right)=\frac{N_0^N}{N!}\,e^{-N_0}$$

Poisson Distribution

$$Po(N, N_0) = \frac{N_0^N}{N!} e^{-N_0}$$

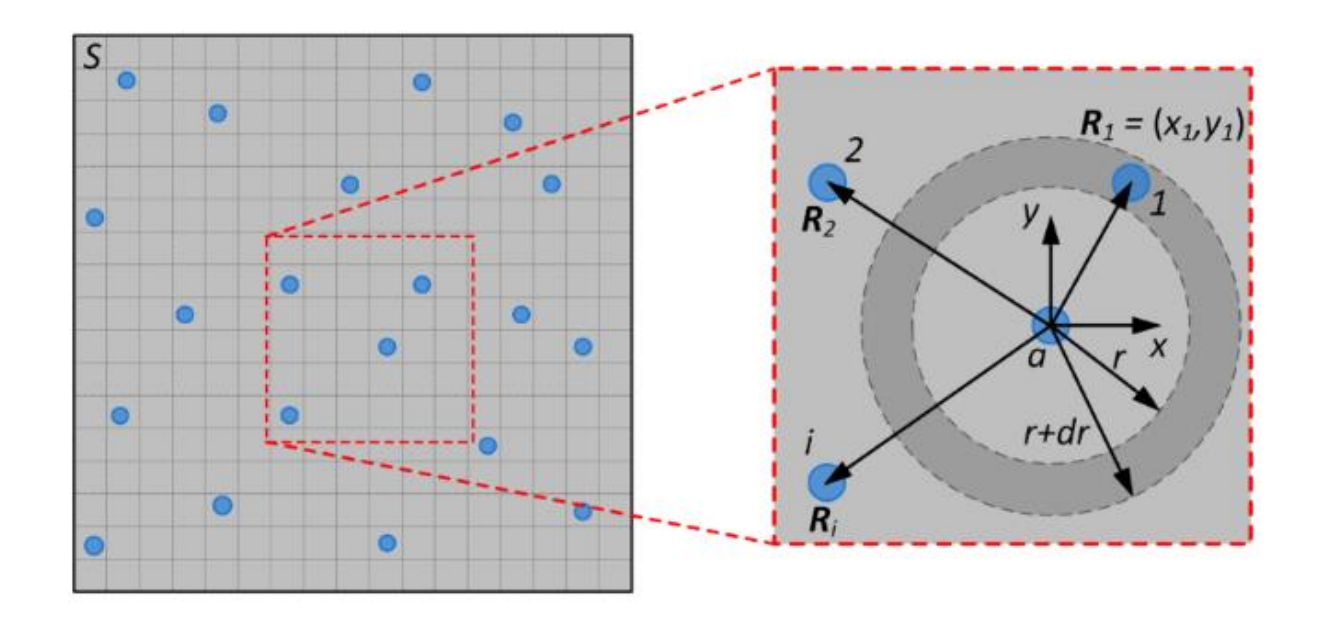
$$\sum_{N=0}^{\infty} P(N, N_0) = \sum_{N=0}^{\infty} \frac{N_0^N}{N!} e^{-N_0} = e^{N_0} \cdot e^{-N_0} = 1$$

What Marks the CHF

- Isolated bubbles dissipate heat better than merged bubbles
- CHF is reached when you have the maximum number of isolated bubbles
- With elevated temperature, more nucleation sites become activated while more bubbles are likely to merge into each other.
- It is important to consider the distance between bubbles



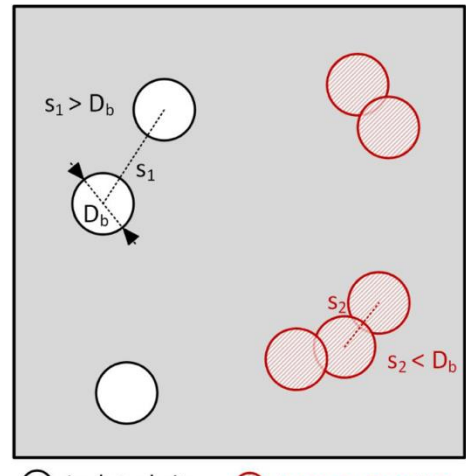
Nearest Neighbor Distance Between Nucleation Sites



The probability distribution function for distance between nearest neighbors if there are N points randomly distributed on a surface of area A

$$f(s) = \frac{2\pi Ns}{A} e^{-\frac{\pi Ns^2}{A}}$$
 Rayleigh distribution

Number of Isolated Bubbles



O Isolated site Interacting site



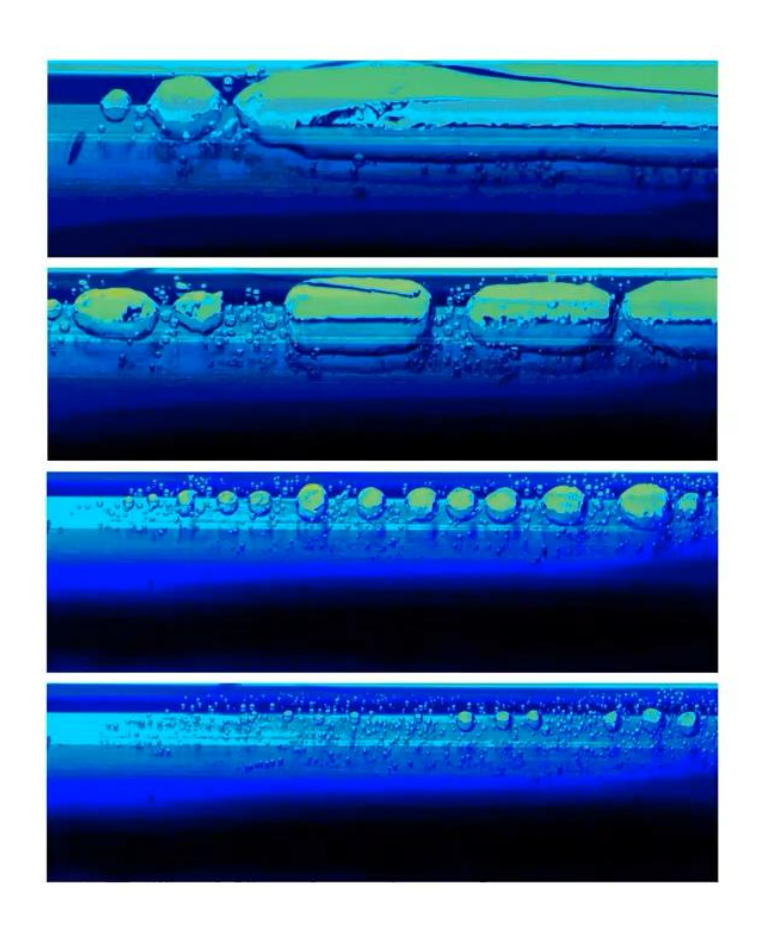
CHF Criteria





- Force balance model for CHF
- Effect of surface parameters on CHF
- Statistical approach for CHF

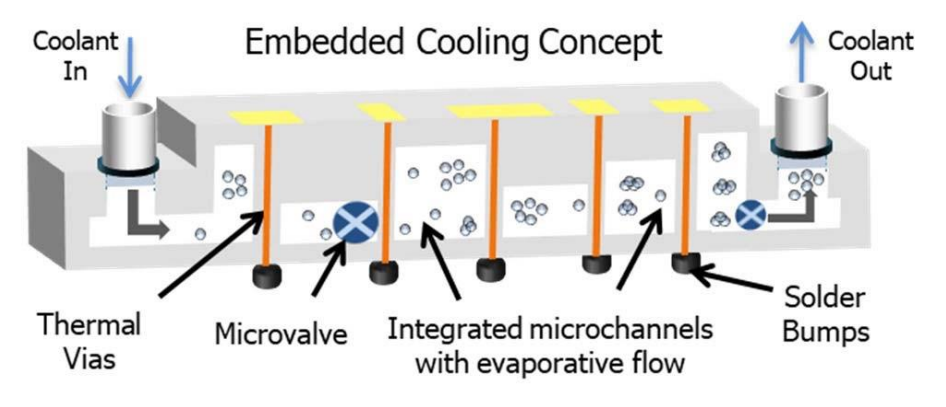
Intro to Flow Boiling



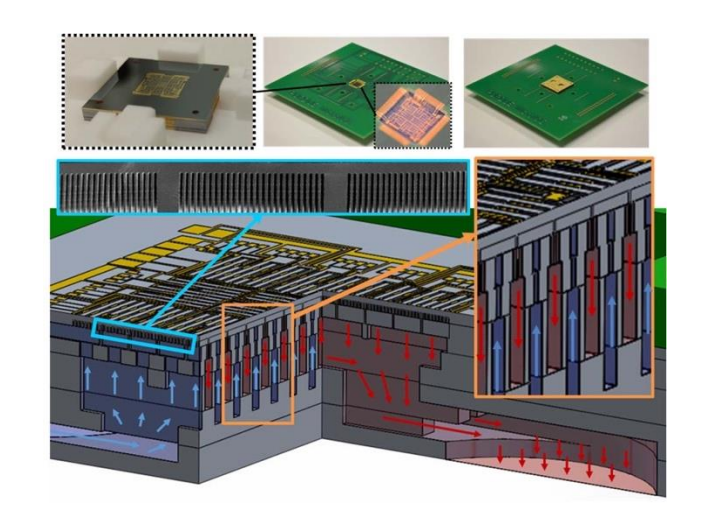
Different regimes in flow boiling (slowed down 50 times)

https://www.youtube.com/shorts/HNcp7zDtwx8?feature=share

Primarily explored for high flux electronics cooling

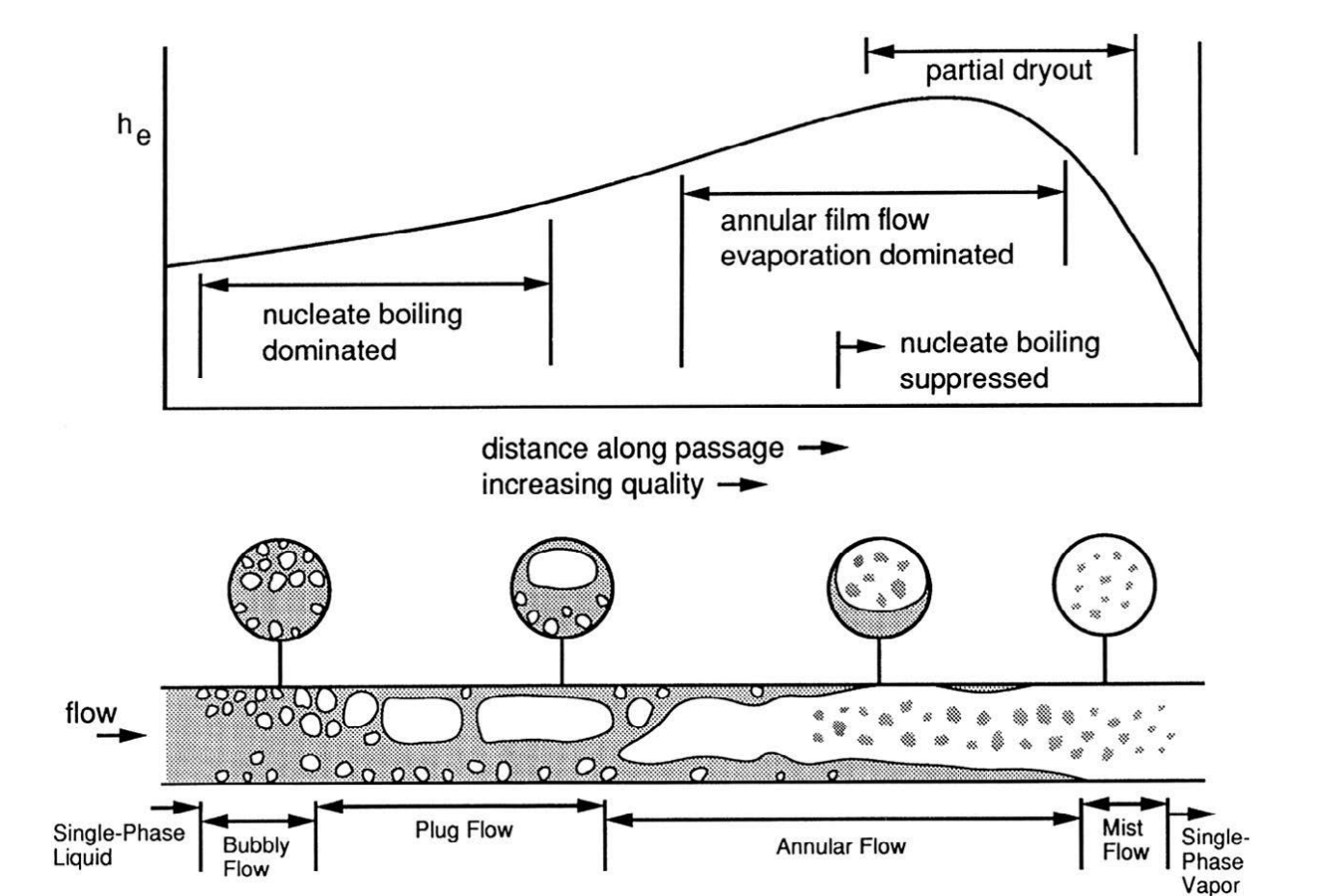


DOI: 10.1109/TCPMT.2021.3111114



International Journal of Heat and Mass Transfer 117 (2018) 319–330

Flow Regimes



Bubbly flow: discrete bubbles dispersed in continuous liquid phase

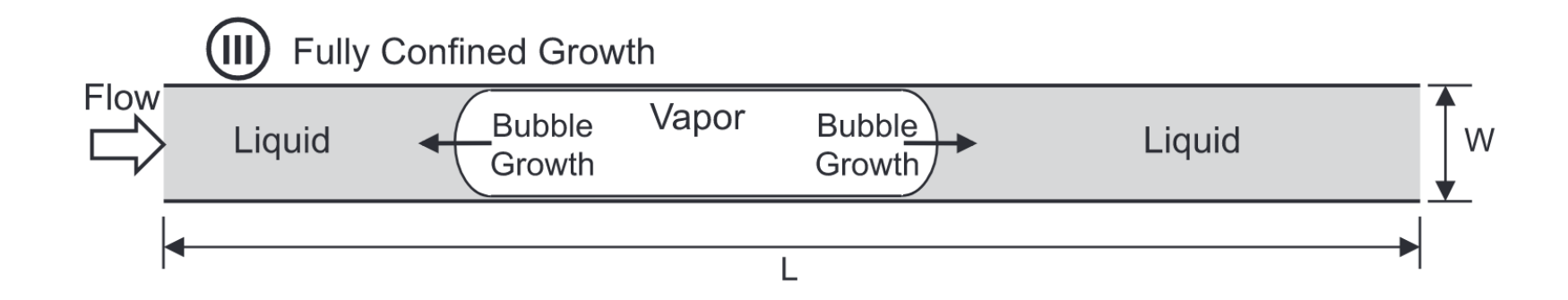
Plug flow: coalescence of small bubbles produces large bubbles flowing in the upper portion

Annular flow: most liquid flowing along the wall and gas flowing in the central core

Mist flow: discrete droplets dispersed in continuous vapor phase

Figure 12.1 in Carey

Oscillations in Microchannel Flow Boiling



Bubble expansion toward the inlet causing density wave oscillation in microchannels

Flow rate reduced (potentially leading to backflow), which gives rise to further vapor expansion toward the inlet

Eventually, liquid rushes back into the channel when sufficient pressure is built up



Density Wave Oscillations in Microchannels

